

Supplementary Materials

Supplementary Discussion

As mentioned in the main text, the plunge-freezing process is unlikely to have reduced the number, length, or positions of the filaments artifactually, since it happens so quickly that even the water in the buffer does not crystallize (Dubochet, 2007). Nevertheless before cells are plunge-frozen, the film of buffer they are suspended in across the EM grid is blotted until it is only slightly thicker than the cells themselves for a fraction of a second before freezing. It is conceivable that the resulting changes in surface tension are somehow communicated through the (intact) cell wall and cause ultrastructural changes, but we judge this unlikely, since the cells are not noticeably flattened (Fig. 9C) and the surface protein and membrane layers are consistently crystalline and smooth, respectively. Microtubules, which are of course related to FtsZ, and many other cytoskeletal filaments both *in vitro* and *in vivo* and in both prokaryotes and eukaryotes have also been seen to remain intact through plunge-freezing (Jensen & Briegel, 2007; Kurner et al, 2004; Nicastro et al, 2006; Sui & Downing, 2006).

Supplementary Methods

Fluorescence microscopy

In order to localize wild-type and mutant forms of FtsZ by fluorescence light microscopy (fLM), we constructed merodiploid strains expressing wild-type FtsZ fused to YFP at a low level under the control of a vanilic acid inducible promoter, P_{vanA} (Thanbichler & Shapiro, 2006). While FtsZ-YFP cannot support cell division, it assembles with FtsZ and allows its tracking by fLM. The FtsZ-YFP strains were constructed by conjugation of pUJ142 (Meisenzahl et al, 1997) carrying wild-type or mutant FtsZ under the control of a xylose-inducible promoter, into strain MT196 (Thanbichler & Shapiro, 2006), which contains a chromosomal copy of *ftsZ-yfp* at the *vanA* locus, $P_{vanA}::ftsZ-yfp$. MT196 was used to create the images for Figure 2. The following growth conditions were used for Figures 2, 4, and S10. 100 μ L aliquots of a frozen overnight

culture were inoculated into 3 ml PYE and grown for approximately 15 hours at 30°C. 75 μ L aliquots from these cultures were inoculated into 3 ml PYE with the appropriate antibiotics and 0.5 mM vanillic acid and grown for three hours at 30°C. 3 μ L was spotted onto a 1% M2G agarose pad supplied with the appropriate antibiotics (Ryan et al, 2002). The strain for Figure 4 was created by conjugating pUJ142FtsZG109S from strain YB1507 into MT196 to create strain YB3538. pUJ142FtsZG109S was conjugated into LS4281 (NA1000 *P_{xyl}::mCherry-mreB*) (Dye et al, 2005) to create the strain YB5003. MT196, YB3538, LS4281, and YB5003 were imaged for Figure S10. A22 was added to the cells 3 hours or 20 min (at the time of induction) before imaging in cells over-expressing FtsZG109S or not, respectively, to match the ECT experiments. 1 mL of the culture was centrifuged for two minutes (4600 x g) and the pellet was resuspended in 100 μ L of the remaining supernatant. For Figure 3, YB3541 was created by conjugating the xylose inducible pUJ142FtsZ (wild-type) plasmid from strain YB1732 into MT196 (Thanbichler & Shapiro, 2006; Din et al, 1998). A fresh colony of YB3541 was inoculated into 3 ml PYE and grown for approximately 15 hours at 30°C. The culture was then diluted to an OD₆₀₀ of 0.1 and grown for an additional three hours. 0.5 mM vanillic acid was added to the culture one hour before viewing on the microscope. Images were acquired on a Nikon Eclipse E800 light microscope using a Nikon 100x Plan Apo Ph3 DM and a DIC H objective with a Princeton Instruments CCD-1317 camera. Images were analyzed using Metamorph versions 6.2 and 7.1.1.0 imaging software. All *C. crescentus* strains were grown in peptone yeast extract (PYE) medium containing 5 μ g/mL kanamycin, 0.5 μ g/mL chloramphenicol, 0.3% xylose, 0.5 mM vanillic acid, and 10 μ g/mL A22 when needed.

Supplementary Movie. The movie is a three-dimensional tour through the ECT reconstructions of four cells: two NA1000 cells and two cells over-expressing FtsZG109S. The NA1000 cells are introduced with a fLM image of YFP-labeled FtsZ in NA1000 cells (labeled "Caulobacter crescentus PvanA::ftsZ-eyfp (MT196)" in the movie), showing that FtsZ normally localizes as a ring at midcell. Next a cryo-EM image of a dividing NA1000 cell is shown, zooming in on the division site which will be reconstructed. The original tilt-series of images is shown (labeled "Tilt Series"), followed by the full 3-D reconstruction (labeled "Tomogram") slice-by-slice. The segmented inner membrane (blue), outer membrane (gold), and FtsZ filaments (red) are then

shown from a range of views while the raw reconstruction is flashed on and off to give the viewer a sense for the interpretability of the data. Next a second NA1000 cell is shown (labeled "Another cell more deeply constricted") in a similar but abbreviated fashion without the tilt series or full reconstruction. The two cells over-expressing FtsZG109S are introduced with another fLM image using FtsZ-YFP (labeled "FtsZ G109S"), showing that FtsZ accumulates in the extended division sites. An additional fly-around of one particular filament and its connection to the cell wall is included (labeled "Connections to peptidoglycan"). Finally the second cell over-expressing FtsZG109S is shown (labeled "Another mutant cell"), wherein an additional cytoplasmic cytoskeletal filament bundle (orange) is seen. Three particularly well-resolved, long filaments that could almost be traced over the top and bottom of the cell were organized as interlaced spirals.

Supplementary References

Dubochet J (2007) The physics of rapid cooling and its implications for cryoimmobilization of cells. *Method Cell Biol* **79**: 7-21

Dye NA, Pincus Z, Theriot JA, Shapiro L, Gitai Z (2005) Two independent spiral structures control cell shape in *Caulobacter*. *Proc Natl Acad Sci U S A* **102**: 18608-18613

Jensen GJ, Briegel A (2007) How electron cryotomography is opening a new window onto prokaryotic ultrastructure. *Curr Opin Struct Biol* **17**: 260-267

Kurner J, Medalia O, Linaroudis AA, Baumeister W (2004) New insights into the structural organization of eukaryotic and prokaryotic cytoskeletons using cryo-electron tomography. *Exp Cell Res* **301**: 38-42

Meisenzahl AC, Shapiro L, Jenal U (1997) Isolation and characterization of a xylose-dependent promoter from *Caulobacter crescentus*. *J Bacteriol* **179**: 592-600

Nicastro D, Schwartz C, Pierson J, Gaudette R, Porter ME, McIntosh JR (2006) The molecular architecture of axonemes revealed by cryoelectron tomography. *Science (New York, NY)* **313**: 944-948

Ryan KR, Judd EM, Shapiro L (2002) The CtrA response regulator essential for *Caulobacter crescentus* cell-cycle progression requires a bipartite degradation signal for temporally controlled proteolysis. *J Mol Biol* **324**: 443-455

Sui H, Downing KH (2006) Molecular architecture of axonemal microtubule doublets revealed by cryo-electron tomography. *Nature* **442**: 475-478

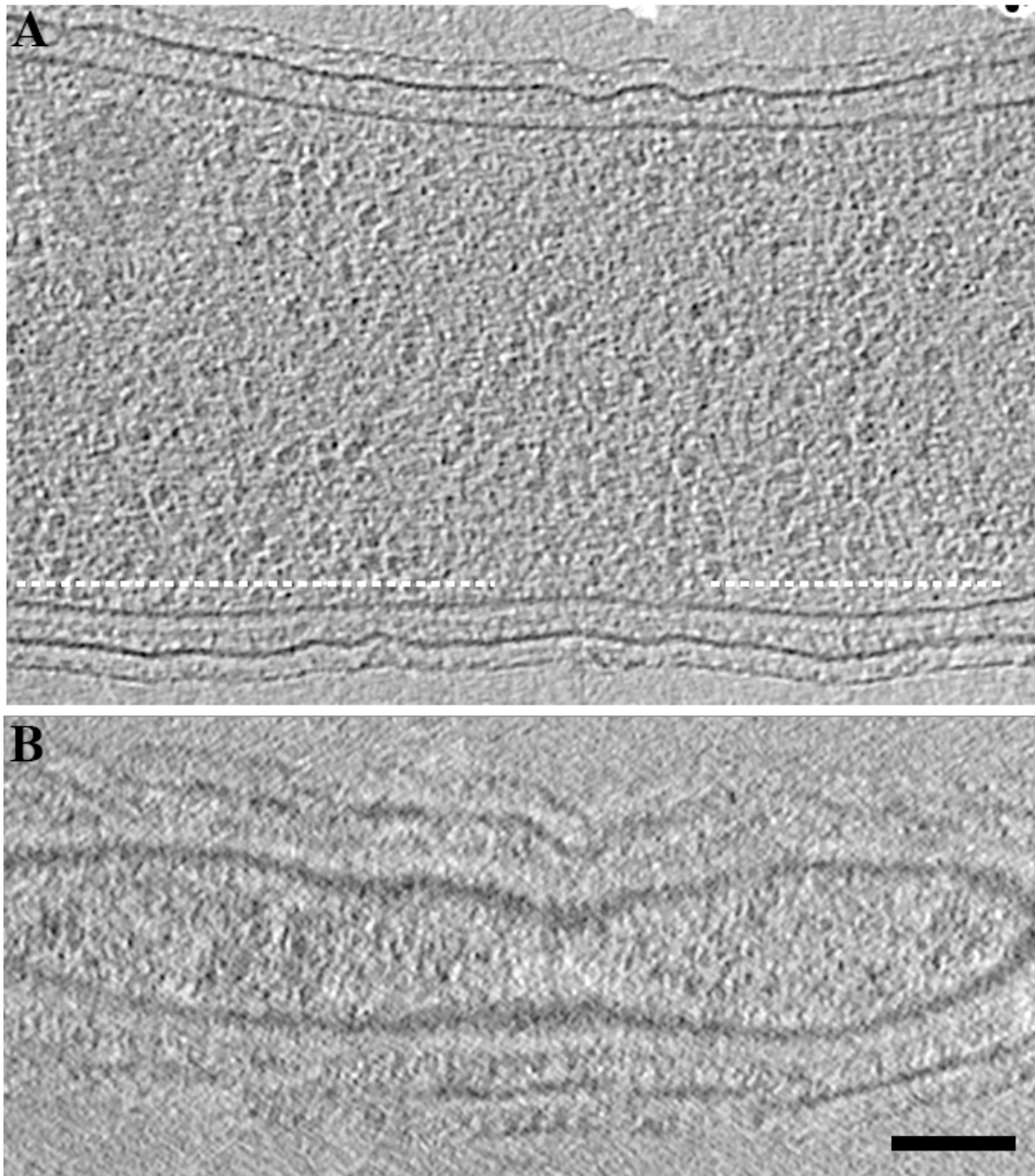


Figure S1

Figs. S1-S7. Raw tomographic slices through the cells shown in Figs. 2A, 2B, 2D, 2E, 2F, 2G, and 5C, respectively. (Panels A) 8 nm slices parallel to the grid. (Panels B) 5.4 nm slices along the dashed lines in (A). White arrows point to arc-like filaments. Scale bars 100 nm. Note that corresponding slices for the cells shown in Figs. 2C and 5A appear in Figs. 1 and S4, respectively.

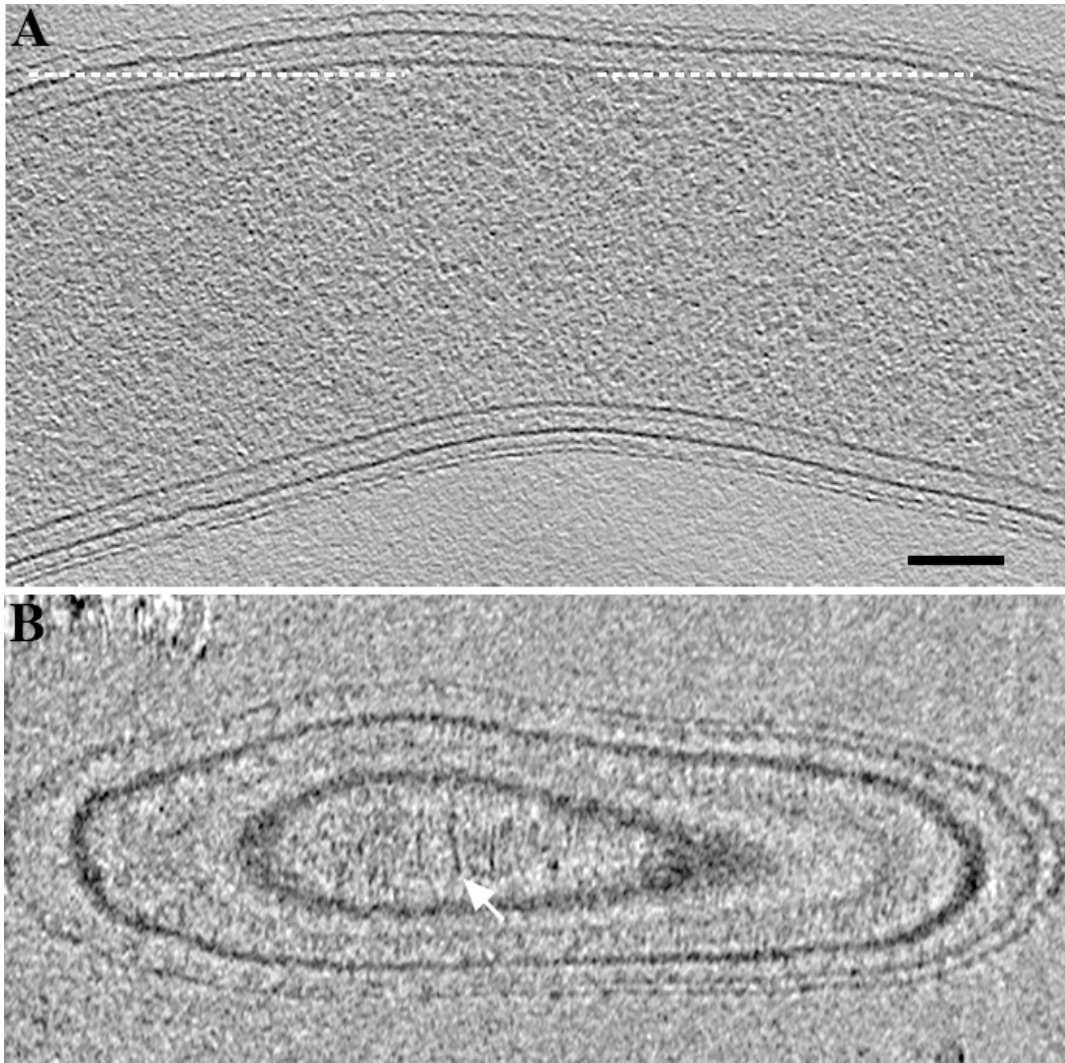


Figure S2

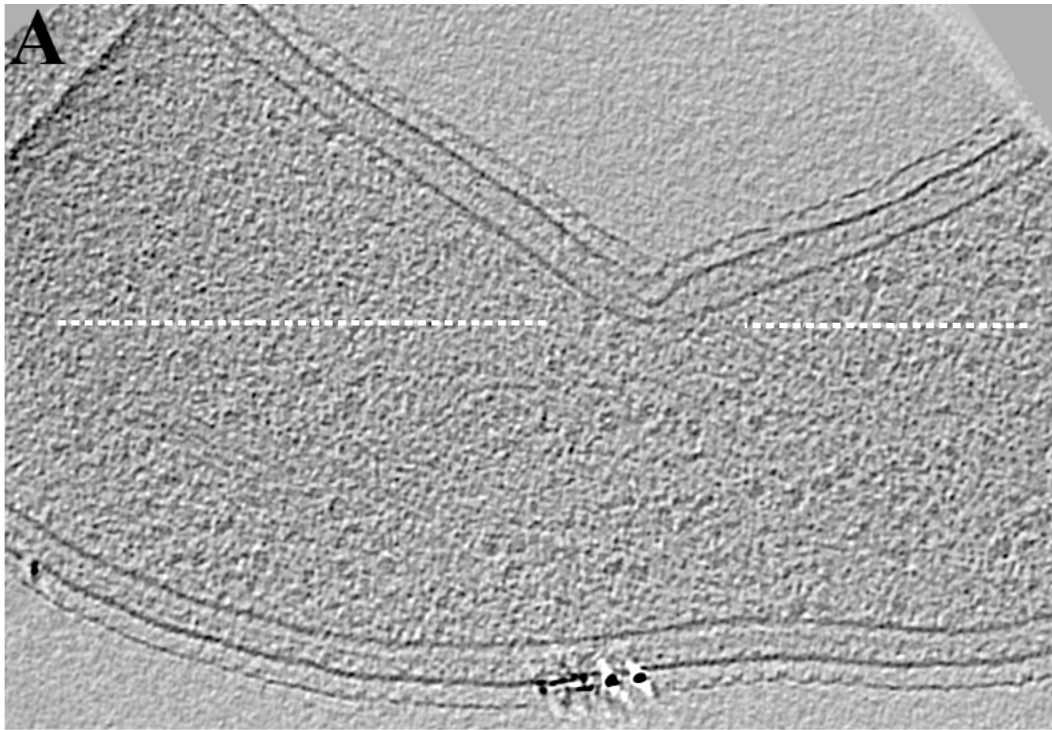


Figure S3

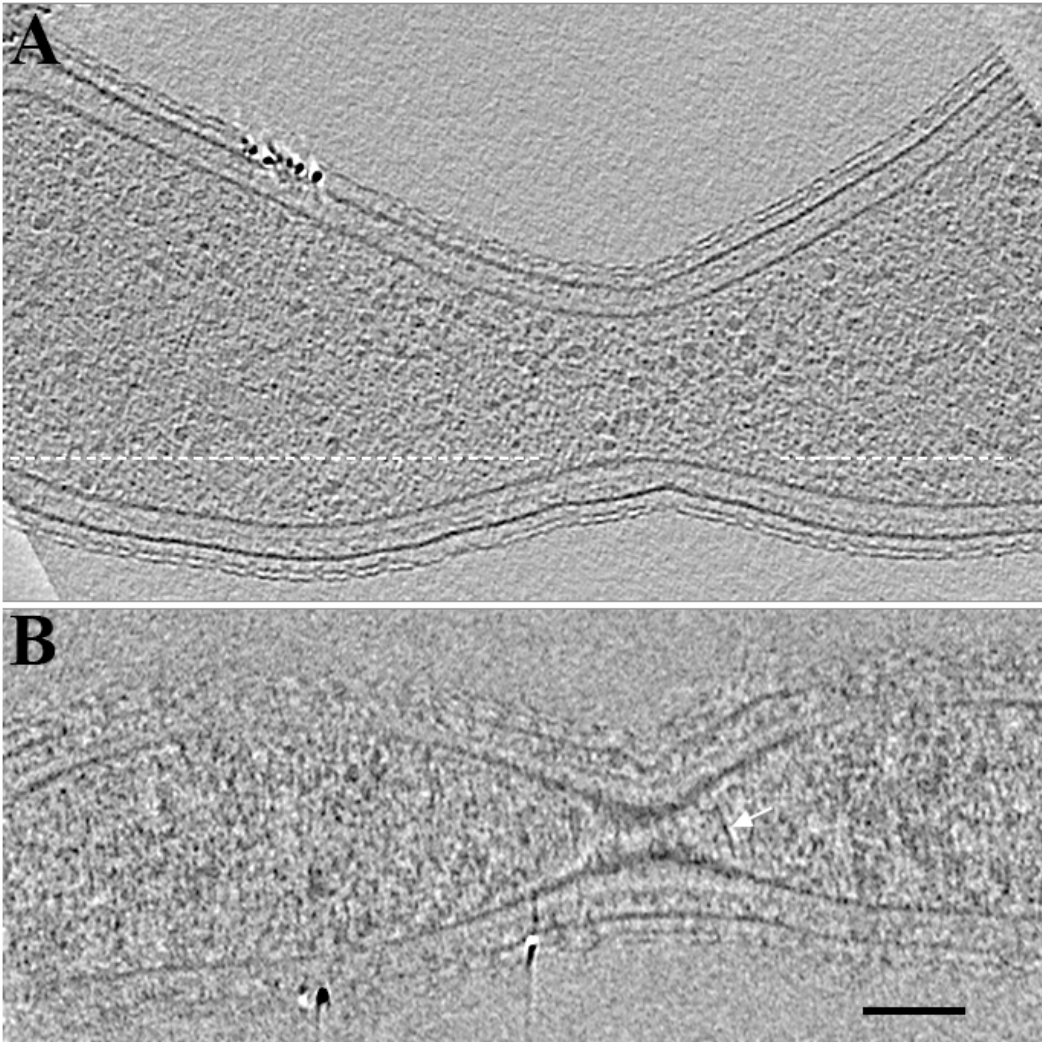


Figure S4

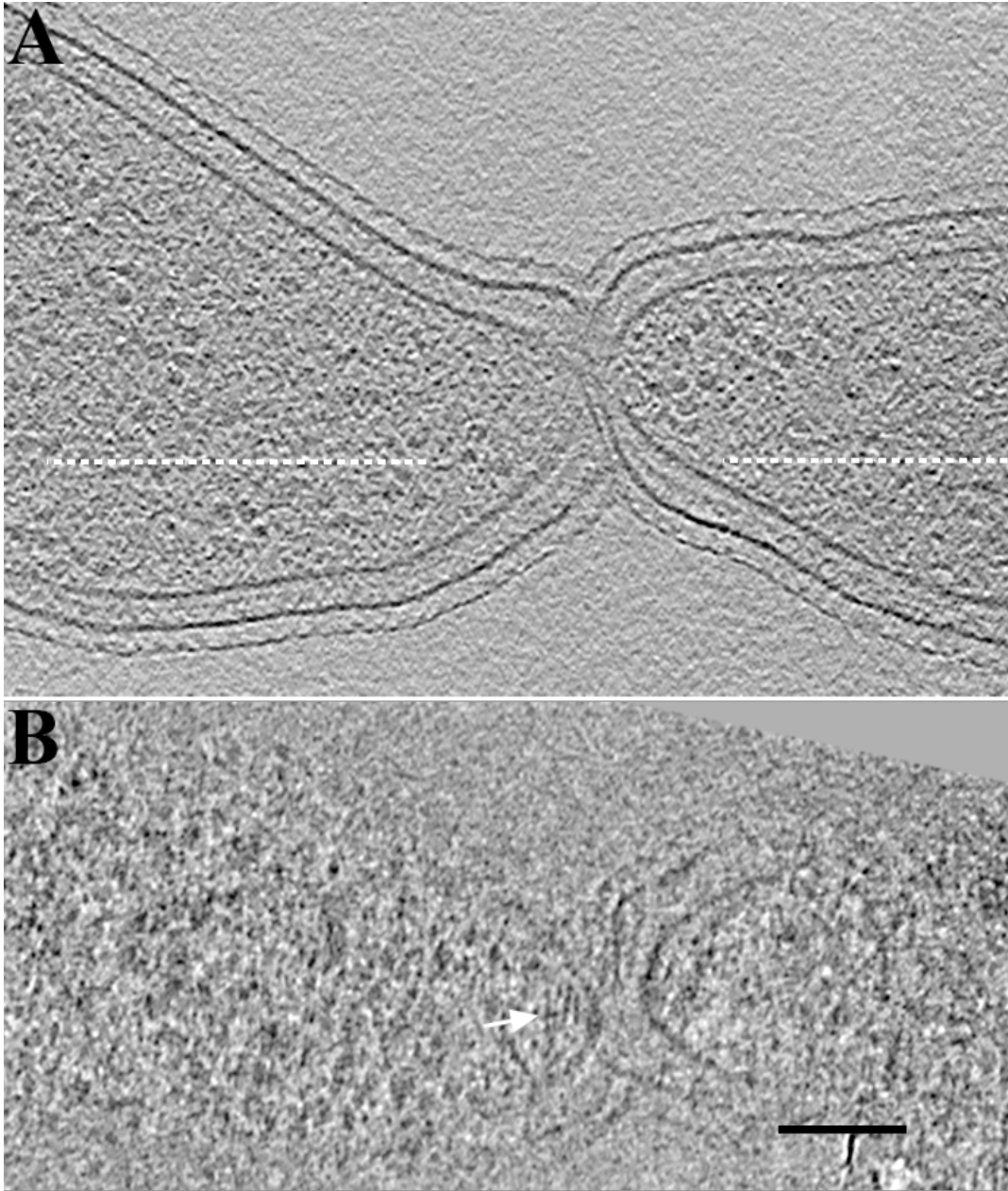


Figure S5

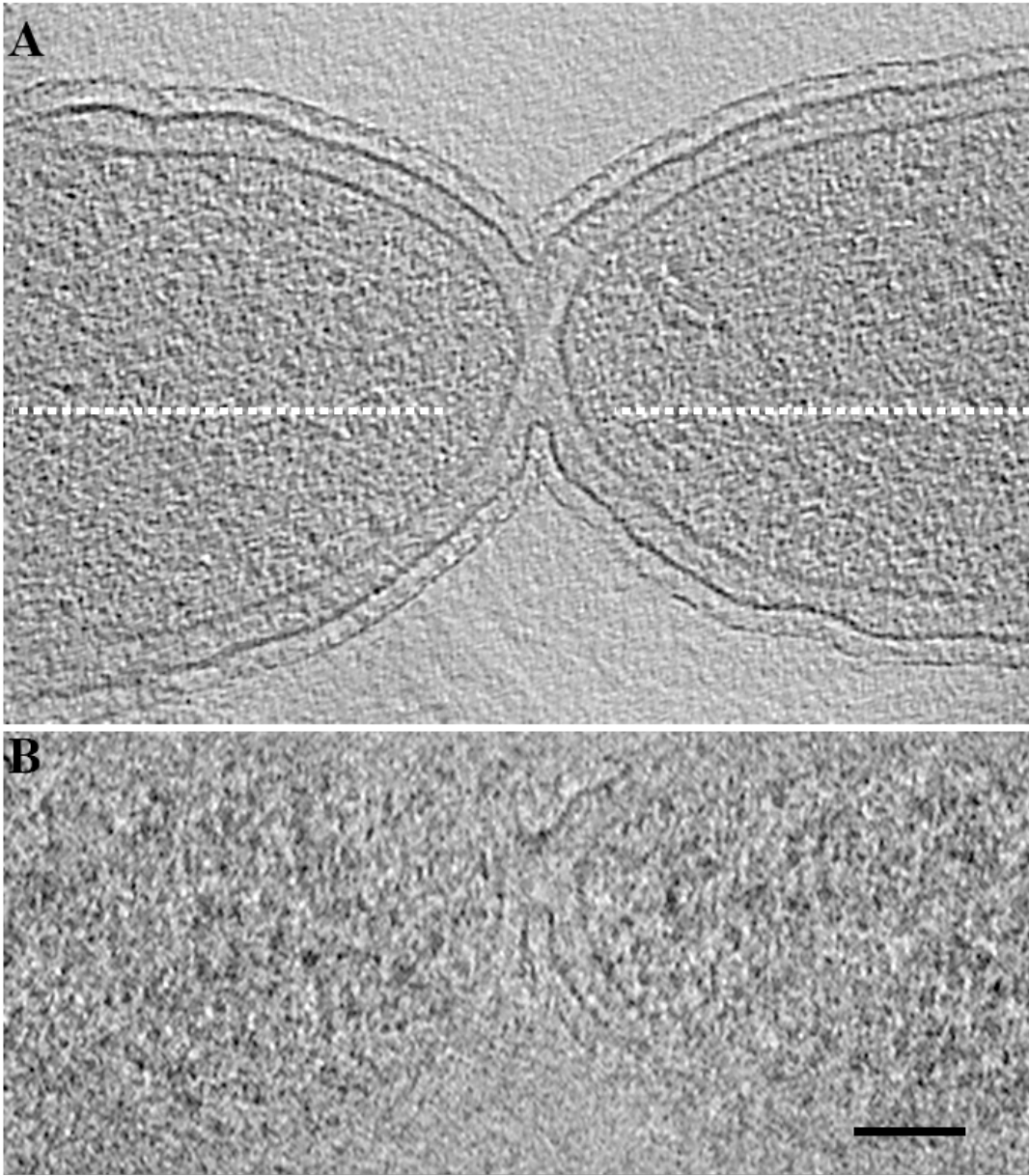


Figure S6

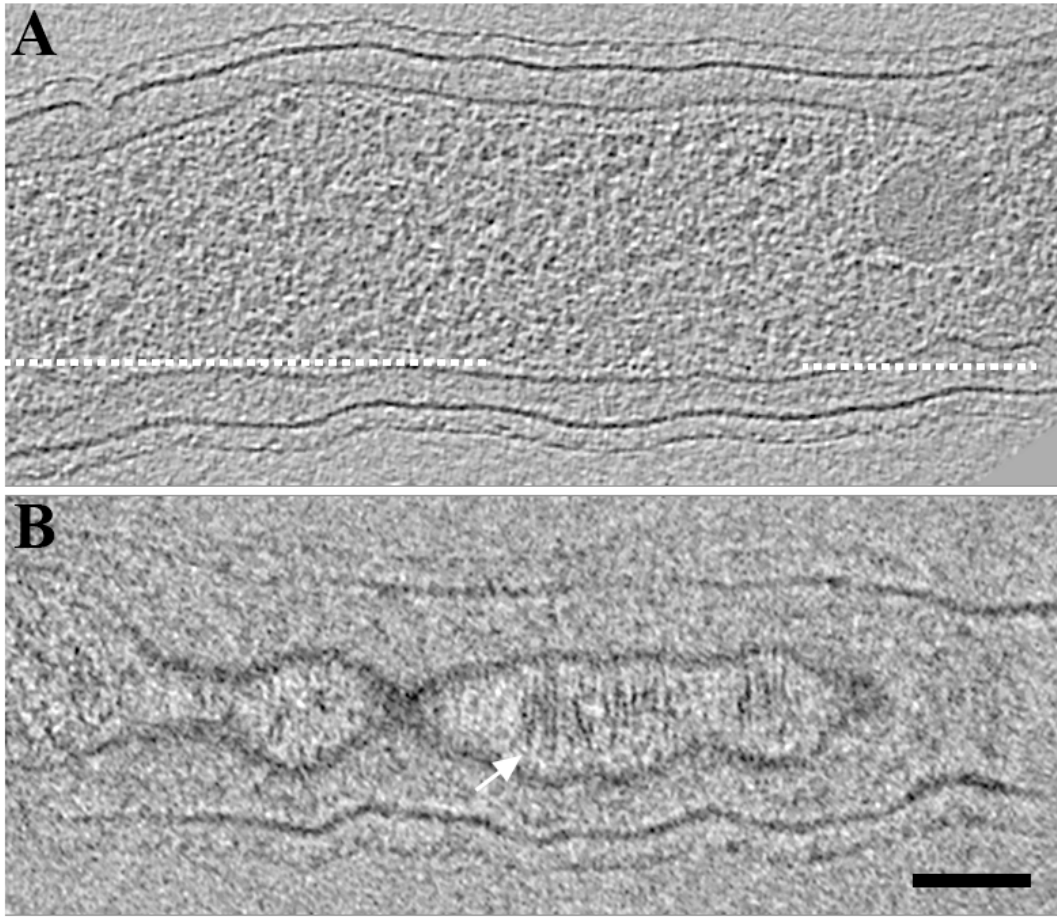


Figure S7

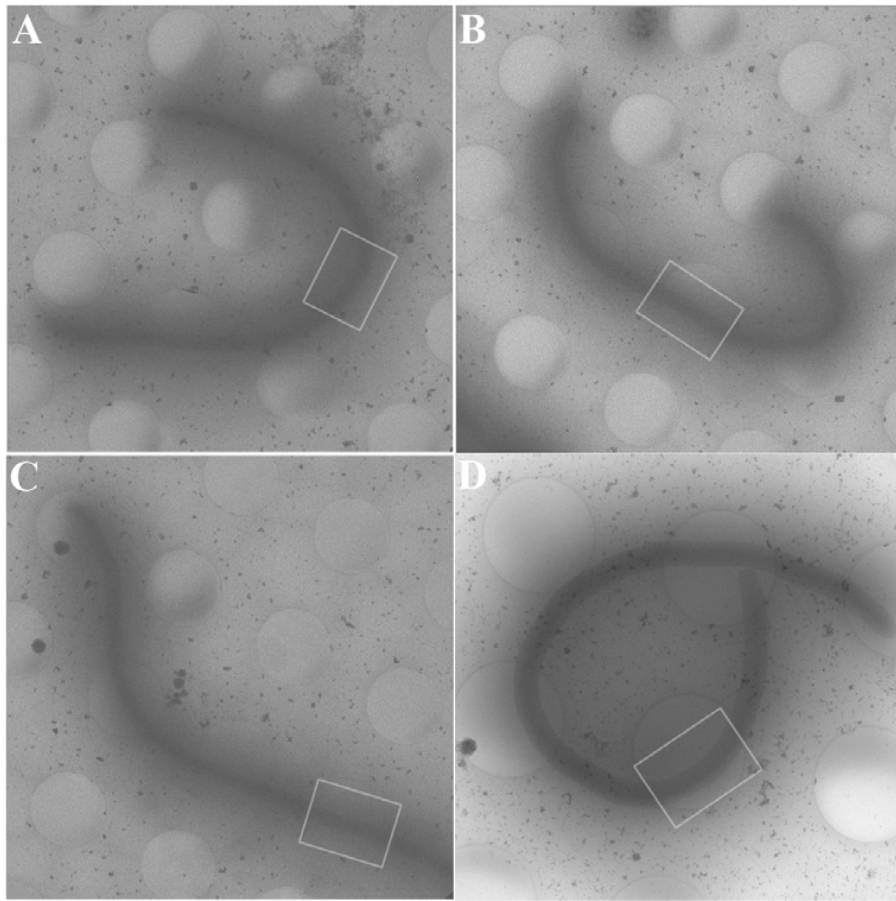


Figure S8

Fig. S8. Low magnification cryo-EM view of four *C. crescentus* YB1585 cells after xylose deprivation for ~6 hours. Note that constriction sites are not visible and it is impossible to image the whole cell at the magnification of 34kx, so random areas along the cell bodies (shown in grey boxes) were imaged by ECT, but no arc-like filaments were seen (Fig. S9). For scale, the diameter of the holes in the carbon support film is 2 μm .

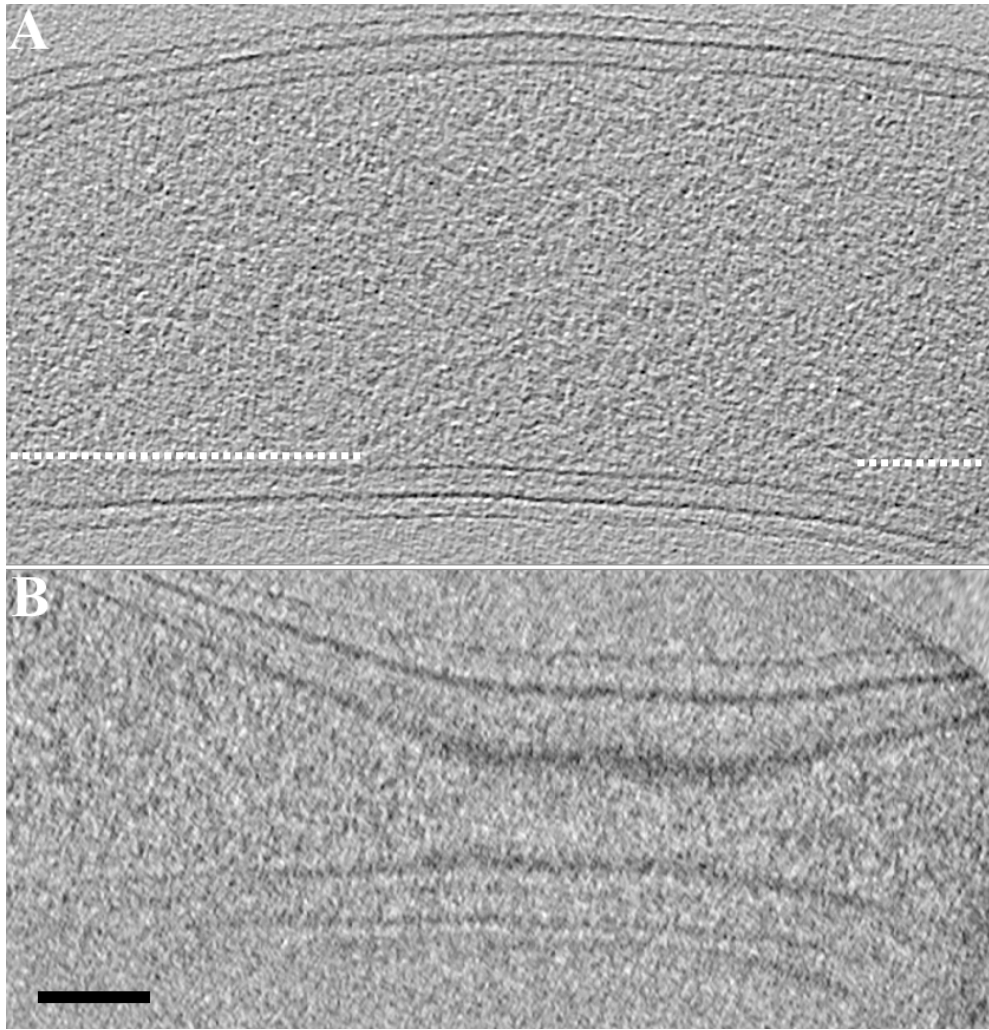


Figure S9

Fig. S9. Absence of arc-like filaments in FtsZ depletion strain YB1585.

Tomographic slices of the cell shown in Supp. Fig. S8, panel D are shown as an example. (A) 8 nm slice parallel to the grid. (B) 5 nm slice along the dash line in (A). Scale bar 100 nm.

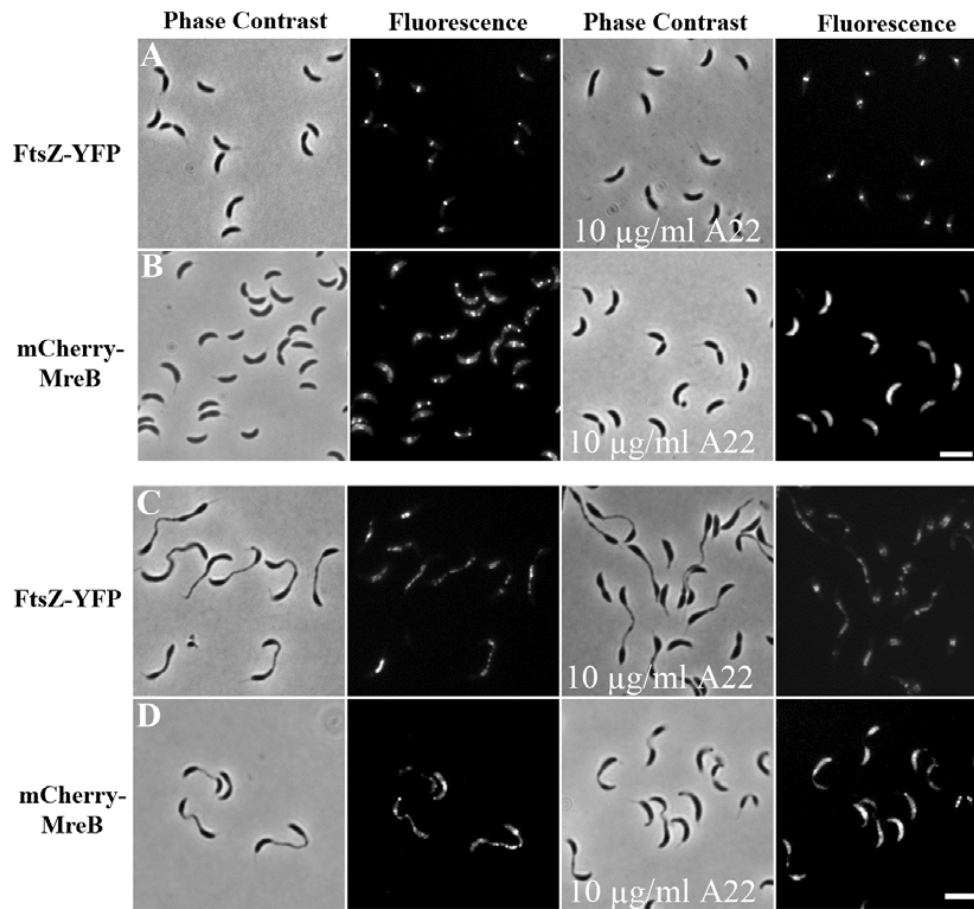


Fig. S10. Arc-like filaments persist in the presence of A22. In support of Fig. 5 of the main text, the expected behaviors of FtsZ and MreB in the presence and absence of A22 were confirmed by fLM. Phase contrast (first and third columns) and fluorescence (second and fourth columns) LM image pairs are shown. The image pairs show cells in the absence (left) and presence (right) of A22. (A) FtsZ-YFP-expressing NA1000 cells, showing that the ring-like localization of FtsZ-YFP is not affected by A22. (B) mCherry-MreB-expressing NA1000 cells, showing that the punctate pattern of MreB in untreated cells is almost completely delocalized by A22. (C) Cells expressing both FtsZ-YFP and FtsZG109S, showing that the patches of FtsZ that appear throughout the extended constriction sites are unaffected by A22. (D) Cells expressing both mCherry-MreB and FtsZG109S, showing that the punctate pattern of MreB seen throughout both the cell bodies and the extended division sites is delocalized by the presence of A22. Scale bar 4 μm .

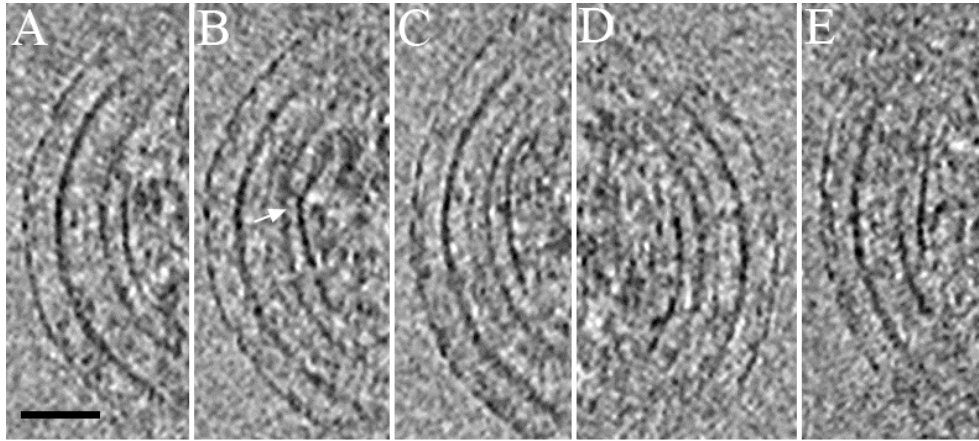


Figure S11

Fig. S11. Straight segments of FtsZ filaments in cells over-expressing (wild-type) FtsZ. 4 nm tomographic slices containing example straight segments and abrupt “kinks” (white arrow). Scale bar 50 nm.